

Complement activation by photooxidation products of A2E, a lipofuscin constituent of the retinal pigment epithelium

Jilin Zhou*, Young Pyo Jang*, So Ra Kim*, and Janet R. Sparrow**†

Departments of *Ophthalmology and †Pathology and Cell Biology, Columbia University, New York, NY 10032

Edited by Nicholas J. Turro, Columbia University, New York, NY, and approved September 19, 2006 (received for review May 23, 2006)

Recent studies have implicated local inflammation and activation of complement amongst the processes involved in the pathogenesis of age-related macular degeneration (AMD). Several lines of investigation also indicate that bis-retinoid pigments, such as A2E, that accumulate as lipofuscin in retinal pigment epithelial (RPE) cells, contribute to the disease process. In an investigation of a potential trigger for complement activation in AMD, we explored the notion that the complex mixture of products resulting from photooxidation of A2E might include a range of fragments that could be recognized by the complement system as “foreign” and that could serve to activate the complement system, leading to low-grade inflammation. To this end, we established an *in vitro* assay by using human serum as a source of complement, and we measured products of C3 activation by enzyme immunoassay. Accordingly, we found that the C3 split products inactivated C3b (iC3b) and C3a were elevated in serum, overlying ARPE-19 cells that had accumulated A2E and were irradiated to induce A2E photooxidation. Precoating of microtiter plates with two species of oxidized A2E, peroxy-A2E, and furano-A2E, followed by incubation with serum, also activated complement. We suggest that products of the photooxidation of bis-retinoid lipofuscin pigments in RPE cells could serve as a trigger for the complement system, a trigger that would predispose the macula to disease and that, over time, could contribute to chronic inflammation. These findings link four factors that have been posited as being associated with AMD: inflammation, oxidative damage, drusen, and RPE lipofuscin.

inflammation | macular degeneration

Retinal pigment epithelial (RPE) cells are considered to be a cellular source for at least some of the material that accumulates in drusen, the extracellular deposits that form at the interface between the RPE and Bruch’s membrane (1). Increasing drusen area is also a risk factor for progression of age-related macular degeneration (AMD) (2); however, the primary stimuli underlying the formation of these deposits is unknown. Besides cholesterol and apolipoproteins B and E, sub-RPE deposits house a number of proteins, some of which, including C3, C5, and C9 (C, complement component), C-reactive protein, clusterin and vitronectin, are associated with inflammatory or immune-mediated processes (3–6). It thus has been hypothesized that drusen form, at least in part, as a result of chronic local inflammation (6). This line of thinking is consistent with reports that AMD susceptibility is associated with a variant in the gene-encoding toll-like receptor 4, a proinflammatory mediator (7), that complement components in drusen promote choroidal neovascularization (5); that the risk of AMD is greater in individuals exhibiting high serum levels of C-reactive protein (8), an inflammatory modulator that when bound to certain ligands can trigger complement activation (9). Importantly, 50% of cases of AMD are linked to variants in the gene-encoding complement factor H, a regulatory protein that suppresses formation of the C3 cleavage enzyme (C3bBb) (10–13). Sequence variants in factor B and in C2 also have been linked to AMD (14). The triggers

responsible for activating complement and local inflammatory events are not known, but infectious agents and sequela related to oxidative processes have been suggested (13, 15).

The complement cascade is an effector system that, upon activation, generates a number of bioactive products, some of which including the complement cleavage products C3a and C5a, trigger inflammatory responses (16–18). Activation of complement can occur by three different pathways, two of these being the classical and alternative pathways. In the classical pathway, activation is initiated by binding of protein C1q, the recognition subunit of the C1 complex, to an activator. Binding of C1q is thought to occur via charge and hydrophobic interactions, and the typical activators are immune complexes; however, bacteria, parasites, transformed cells, DNA, and C-reactive protein-associated complexes also serve as activating substances (16–19). Activation of the C1 complex eventually leads to enzymatic cleavage of C4 and then C2, with the C4b and C2a fragments forming the C3 cleavage enzyme (convertase; C4b2a) of the classical pathway. Cleavage of C3, the most important of the C components, enables formation of C4b2a3b, the convertase of C5, which is the first of the components (C5–9) that forms the membrane attack complex.

Activation of the alternative pathway begins with binding of C3b to an activating surface. Once attached to the activator, C3b binds factor B, presents it for cleavage by fluid-phase factor D, and C3bBb, the C3-cleaving enzyme (C3-convertase), is formed. C3bBb cleaves additional C3 leading to amplification of the complement cascade. The molecule of C3b that instigates alternative pathway activation can be produced by the C3 convertase (C4b2a) of the classical pathway. Alternatively, it is generated at a slow rate by a constitutive process that, in the absence of cleavage, changes the conformation of C3 [C3(H₂O) or C3i] such that it is able to bind factor B. This latter process (“tickover”) is mediated by small nucleophiles or water that gain access and react with the internal thioester of C3, rendering it able to form the C3 convertase with factor B (in the presence of factor D), thus initiating C3b formation (20). All told, in addition to pathogens and immune complexes, complement activation can be triggered by stimuli as diverse as oxidatively modified low-density lipoproteins (21, 22), amyloid-β (23), polyethylene implants (24, 25), and carbon nanotubes (26). The structural features that determine whether

Author contributions: J.Z. and Y.P.J. contributed equally to this work; J.R.S. designed research; J.Z., Y.P.J., and S.R.K. performed research; J.Z., Y.P.J., S.R.K., and J.R.S. analyzed data; and J.R.S. wrote the paper.

The authors declare no conflict of interest.

This article is a PNAS direct submission.

Abbreviations: AMD, age-related macular degeneration; atRAL, *all-trans*-retinal; atRAL d-PE, *all-trans*-retinal dimer-phosphatidylethanolamine; C, complement component; iC3b, inactivated C3b; PE, phosphatidylethanolamine; photoox-A2E, photooxidized A2E; RPE, retinal pigment epithelium.

†To whom correspondence should be addressed. E-mail: jrs88@columbia.edu.

© 2006 by The National Academy of Sciences of the USA

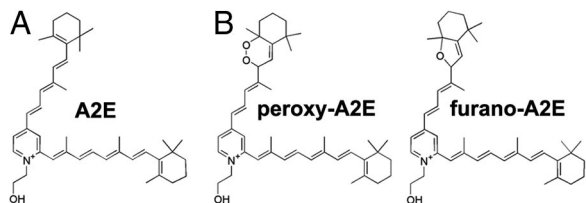


Fig. 1. Structures of the RPE lipofuscin pigment A2E (A) and the monoperoxy-A2E and monofurano-A2E (B) photooxidized forms of A2E.

activation and amplification will occur are not clear, but particle surfaces bearing hydroxyl (-OH) and amine (-NH₂) nucleophiles increase the potential for activation (16–18, 20).

There often has been speculation of a possible association between the amassing of lipofuscin in RPE cells and drusen formation, but such a relationship has not been established. There is considerable variability amongst individuals in terms of the extent of the accumulation of RPE lipofuscin, but the most abundant accretion is in the RPE cells underlying central retina (27). The most intensely studied of the RPE lipofuscin pigments are the bisretinoid compounds A2E (Fig. 1), iso-a2E and the minor cis isomers of A2E, all of which have absorbance maxima in the blue region of the spectrum (28, 29). A2E formation begins in photoreceptor outer segments from inadvertent condensation reactions between phosphatidylethanolamine (PE) and *all-trans*-retinal (atRAL) (1:2) that generate A2-PE, the immediate precursor of A2E (29–31). A2-PE is deposited in RPE cells during the normal process of outer-segment phagocytosis and subsequent phosphate cleavage of A2-PE generates A2E. Other products of reactions of *all-trans*-retinal are *all-trans*-retinal dimer-phosphatidylethanolamine (atRAL d-PE) and its cleavage product atRAL dimer-ethanolamine, both of which have been isolated from the lipofuscin-filled RPE of *Abca4/Abcr* null mutant mice and in RPE isolated from human donor eyes (32). Besides having structures that are distinct from A2E, atRAL d-PE and atRAL

dimer-ethanolamine have UV-visible absorbance spectra that are red-shifted relative to A2E (atRAL d-PE: λ_{\max} 265, 510; A2E: λ_{\max} 335, 439).

The photoreactivity of RPE lipofuscin has been of immense interest to investigators for some time (33). In the case of A2E, 430-nm irradiation leads to the generation of singlet oxygen and superoxide anion (34–36). A2E is also an efficient quencher of singlet oxygen such that the carbon–carbon double bonds situated along the retinoid-derived side arms of A2E become oxidized, forming a mixture of oxygen-containing moieties including epoxides, furanoid oxides, and cyclic peroxides (36–38), at least some of which are likely highly reactive (39, 40). By mass spectrometry, products of photooxidized A2E (photooxo-A2E) present as a series of $m/z + 16$ peaks starting from the M⁺ m/z 592 peak (A2E). We have isolated monofurano-A2E and monoperoxy-A2E (Fig. 1) in ARPE-19 cells that have accumulated A2E and are irradiated at 430 nm, and both have also been detected in RPE from aged human and in eyecups from mice with null mutations in *Abca4/Abcr* (37), the gene responsible for recessive Stargardt disease (41).

Here, we explore the possibility that products of the photooxidation of RPE lipofuscin pigments could serve as a triggering factor for the complement system, a trigger that would predispose the macula to disease and that could generate the low-grade complement activation that, over time, contributes to the chronic inflammatory processes underlying drusen formation. Because it is impractical to measure complement activation at the RPE-Bruch's membrane interface in the eye, we constructed *in vitro* models that employ complement in human serum to assay under cellular and noncellular conditions.

Results

iC3b Generation by Photooxidation Products of A2E. In these experiments, human serum was used as a source of complement (26), and as a first approach, we assessed complement activation by measuring fluid-phase C in serum placed in contact with ARPE-19 cells that had accumulated A2E and were irradiated at 430 nm to generate photooxo-A2E products. A2E photooxi-

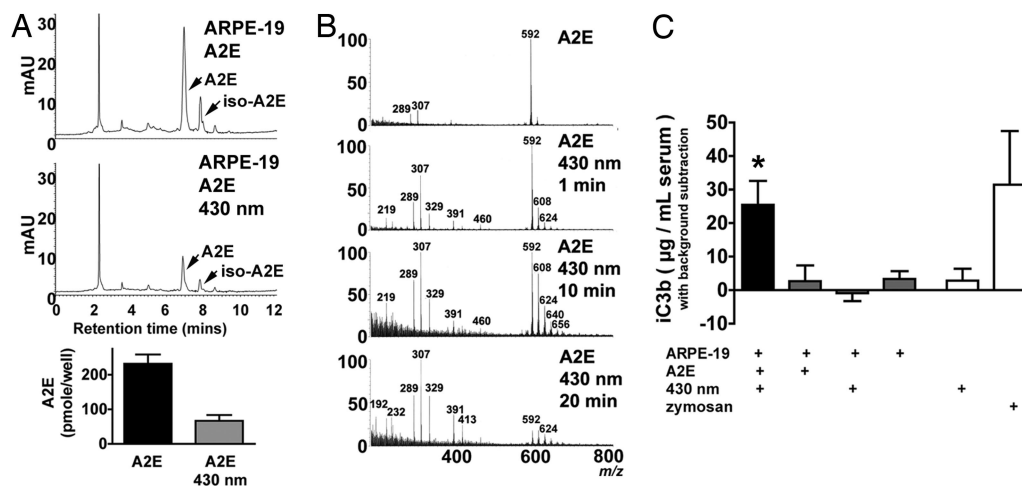


Fig. 2. A2E photooxidation and iC3b generation. (A) Reverse-phase HPLC detection of A2E in extracts of ARPE-19 cells that accumulated A2E (ARPE-19 A2E) and cells that accumulated A2E and were irradiated for 30 min (ARPE-19 A2E 430 nm). (A Top and Middle) Reductions in peak height under conditions of 430-nm irradiation are indicative of A2E photooxidation. (A Bottom) HPLC quantitation illustrates photooxidation-associated reduction of A2E in irradiated cells. Mean \pm SEM of three to six values. (B) FAB-MS spectrum of nonirradiated sample of A2E (m/z 592) and A2E after irradiation at 430 nm for 1, 10, and 20 min. Photooxidation of A2E is evidenced by a reduction in the molecular ion peak at m/z 592 (A2E) and by the appearance of m/z 608, 624, 640, and 656 [m/z 592 + (n)16] peaks. After 20 min of irradiation, the decrease in intensity and/or loss of peaks at m/z 608, 624, 640, and 656 reflects fragmentation of photooxo-A2E. (C) iC3b content is elevated in serum overlying (37°C for 2 h) ARPE-19 cells that had accumulated A2E and were irradiated (A2E 430 nm) to generate A2E photooxidation products. Measurement was by enzyme immunoassay. Zymosan incubated in serum at 37°C served as the positive control. Values from undiluted human serum incubated in empty wells at 37°C were subtracted as background. Means \pm SEM, three to eight experiments; *, $P < 0.05$ as compared with ARPE-19 with A2E, ARPE-19 with 430-nm irradiation, or ARPE-19 only.

datation was monitored in companion cultures by extracting the cells in chloroform-methanol and analyzing by reverse-phase HPLC. The HPLC profile revealed a decrease in the absorbance of the A2E peak indicative of photooxidation and consumption of A2E (Fig. 2A). Photooxidation of A2E also was demonstrable when samples of A2E (m/z 592) were irradiated at 430 nm and examined by FAB-MS (Fig. 2B). When irradiation was delivered for 1 and 10 min, A2E photooxidation was evidenced by the appearance of peaks at m/z 608, 624, 640, and 656 [m/z 592 + (n)16] along with diminished intensity of m/z 592. Moreover, the decrease in intensity or loss of these peaks when irradiation was continued for 20 min is attributable to fragmentation of photooxo-A2E as oxidation proceeds. The O–O bonds of endoperoxide moieties in photooxo-A2E are likely sites for cleavage (37).

To monitor C3 cleavage in the overlying serum, we began by measuring iC3b generation by using enzyme immunoassay. iC3b is a fluid-phase product of C3 activation within both the classical and alternative pathways; it forms when C3b is cleaved by factor I (16). Background levels of complement activation, determined by measuring iC3b after incubating serum in empty wells (2.5 h, 37°C; concurrent with the irradiation and incubation of cell-associated samples) were found to be 71.9 (± 3.8 $\mu\text{g}/\text{ml}$) and, thus, severalfold greater than when serum was maintained on ice (3.8 ± 0.3 $\mu\text{g}/\text{ml}$). Complement activation under these conditions was probably due, at least in part, to contact with the polystyrene surface of the well. Subsequently, background levels were determined independently for each experiment and were subtracted from all other values.

Enzyme immunoassay also revealed that iC3b levels in serum overlying irradiated-A2E-laden-ARPE-19 cells were consistently higher than in serum maintained in contact with nonirradiated-A2E-laden-ARPE-19 cells ($P < 0.05$) (Fig. 2C). The elevations in iC3b were prevented when EDTA (10 mM), an inhibitor of both the classical and alternative pathways, was added to serum before irradiation (data not shown). To control for complement activation from other sources, we also measured iC3b generation under conditions in which serum covered ARPE-19 cells that were irradiated in the absence of A2E and ARPE-19 that had not accumulated A2E and were not irradiated; statistically significant differences were not observed ($P > 0.05$). Levels of iC3b generated in the presence of zymosan, a yeast cell wall extract and potent activator of both the alternative and classical pathways (26), were consistently higher than with irradiated A2E-laden RPE.

C3a Formation. To further monitor C3 cleavage, we measured the production of C3a-desArg by enzyme immunoassay. C3a is generated by C3 cleavage and then is converted rapidly by carboxypeptidase N in serum to the more stable C3a-desArg (17); detection of the latter is a reliable indicator of C3a generation via the classical and alternative pathways. The kinetics of C3a production are shown in Fig. 3A. In human serum overlying ARPE-19 cells that had accumulated A2E and were irradiated at 430 nm to generate A2E photooxidation products, activation of complement occurred. There was a steady rise in C3a content when serum incubation was continued for 30–120 min after irradiation. During the same time period, C3a also increased in serum overlying ARPE-19 cells irradiated in the absence of A2E, but levels of C3a were higher in the samples contacting irradiated A2E-containing cells. By selecting a 2-h postirradiation incubation interval for further studies, we compared C3a levels generated in serum under various conditions (Fig. 3B). C3a in serum-covering irradiated A2E-laden ARPE-19 cells was repeatedly higher than C3a in serum-contacting nonirradiated A2E-laden ARPE-19

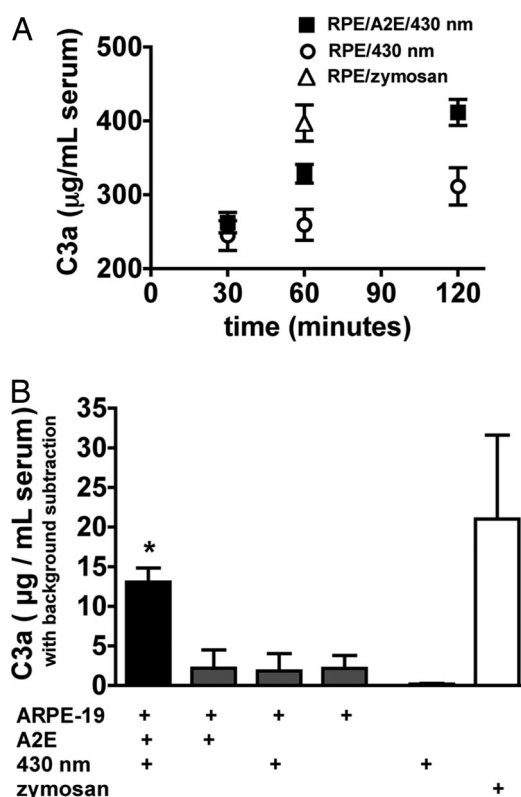


Fig. 3. C3a levels in serum placed in contact with ARPE-19 cells that had accumulated A2E and were irradiated at 430 nm. Measurement by enzyme immunoassay. (A) Time course of formation of C3a. ARPE-19 cells that had accumulated A2E were incubated with undiluted serum at 37°C for 2 h after 430-nm irradiation (RPE/A2E/430 nm). Levels are compared with irradiated cells in the absence of A2E (RPE/430 nm) and to serum with added zymosan (RPE/zymosan). (B) ARPE-19 cells that had accumulated A2E were incubated with undiluted serum at 37°C for 2 h after 430-nm irradiation. Zymosan incubated in serum at 37°C served as the positive control. Values obtained from samples of undiluted human serum incubated in an empty well at 37°C were subtracted as background. Mean \pm SEM of two to four experiments; *, $P < 0.05$ as compared with ARPE-19 with A2E, ARPE-19 with 430-nm irradiation, or ARPE-19 only.

cells ($P > 0.05$) and cells irradiated in the absence of A2E ($P > 0.05$).

iC3b with Peroxy-A2E and Furano-A2E. It could be argued that complement is not activated directly by A2E photooxidation products but instead by other molecular modifications (e.g., advanced glycation end products) that are known to form downstream from photooxidation events initiated by A2E in cells (42). To probe for complement activation under conditions involving direct contact with A2E, peroxy-A2E, and furano-A2E, we synthesized these compounds for introduction to serum in solid form. Reverse-phase HPLC analysis of the products eluting from the reactions of A2E with 1,4-dimethylnaphthalene endoperoxide and A2E with MCPBA (*meta*-chloroperoxybenzoic acid) confirmed the compounds to be peroxy-A2E and furano-A2E (37), respectively: The chromatographic profiles indicated compounds more polar than A2E, hypsochromic shifts (peroxy-A2E, λ_{max} 298, 434; furano-A2E, λ_{max} 297, 433) relative to A2E (λ_{max} 337, 439) reflected oxidations at double bonds, and the molecular mass (m/z 624) was corroborative for the addition of two oxygen atoms in the case of peroxy-A2E and a single oxygen atom in the case of furano-A2E (m/z 608) (Fig. 4A and B).

By enzyme immunoassay, iC3b levels were elevated in serum incubated at 37°C in wells precoated with 156 $\mu\text{g}/\text{cm}^2$ peroxy-

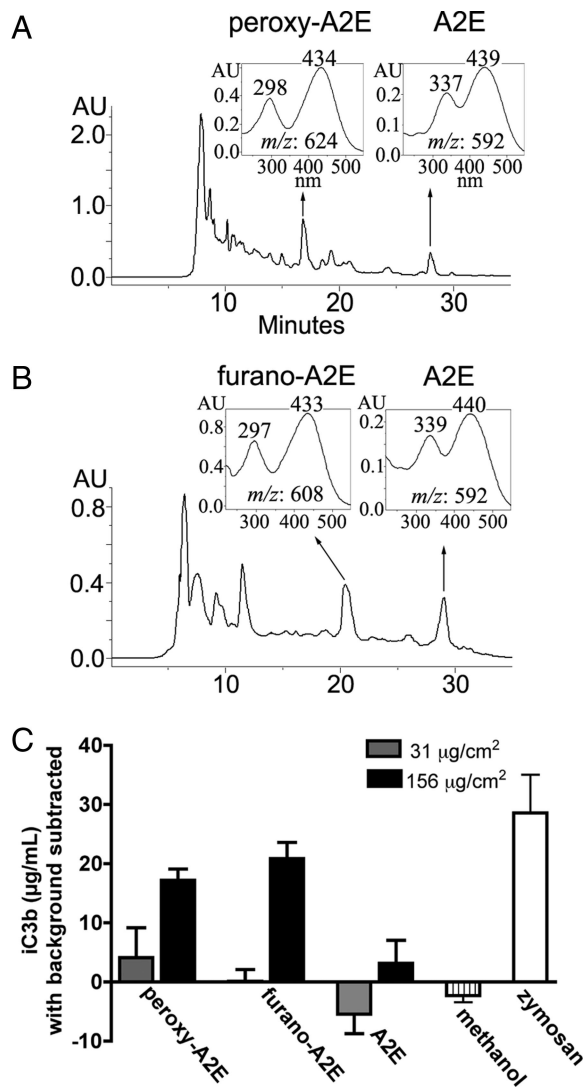


Fig. 4. iC3b generated in serum incubated with solid-form peroxy-A2E and furano-A2E. (A and B) Reverse-phase HPLC detection of peroxy-A2E (A) and furano-A2E (B) after synthesis. UV-visible absorbance spectra (A Insets and B Insets) reveal hypsochromic shift (≈ 40 nm relative to A2E) in the longer wavelength peak, which is indicative of oxidation. Mass (m/z) was assigned by LC-MS with electrospray ionization. (C) iC3b levels in serum that was incubated in wells of a microtiter plate precoated with peroxy-A2E, furano-A2E, and A2E (31 or 156 $\mu\text{g}/\text{cm}^2$). iC3b levels measured in undiluted human serum that had been incubated in an empty well at 37°C were subtracted as background. A suspension of zymosan in serum served as the positive control. iC3b was measured by enzyme immunoassay. Means \pm SEM of three experiments. *, $P < 0.05$ as compared with solvent (methanol) control.

A2E and furano-A2E as compared with the methanol-only control ($P < 0.05$). No change in iC3b levels was observed at the lower concentration. There was also no difference in iC3b content when serum was incubated in wells coated with A2E. iC3b levels measured in serum incubated in an adjacent empty well were used for background subtraction. Suspensions of zymosan in serum produced levels of iC3b that were ≈ 2 -fold greater than with peroxy-A2E and furano-A2E.

Discussion

It was proposed a few years ago that drusen forms as a product of local inflammatory processes (1, 6). More recently, associations between DNA sequence variants in complement factor H, factor B, and C2 have been identified that either confer

protection or risk for AMD (10–14), thus implicating aberrant complement regulation in the presence of an activating agent as an underlying cause of the inflammation. A question of importance pertains to the trigger for the complement-associated events. We have shown here that the photooxidation of A2E in ARPE-19 cells leads to the activation of complement. In addition, exposure of complement-containing serum to peroxy-A2E and furano-A2E, oxidized forms of A2E, also resulted in elevated levels of iC3b, a product of C3 activation that is present in drusen (13). Bisretinoid lipofuscin pigments such as A2E are deposited in the RPE of all individuals, although studies of fundus autofluorescence demonstrate considerable differences in the amount of material accumulated by age-matched subjects (27). The most pronounced accumulation of RPE lipofuscin occurs in central retina (27). The amphiphilic structure of A2E conferred by two retinoid-derived arms connected through a pyridinium ring is unprecedented. Because A2E accumulates, it appears not to be recognized by lysosomal enzymes of the RPE.

Invading pathogens also have been suggested as initiating agents in complement-mediated events underlying AMD (13), but infection may not explain readily why the disease process has a predilection for the macula. On the other hand, the evidence that photooxidation events associated with RPE lipofuscin contribute to AMD pathology is consistent with a role for oxidative mechanisms in AMD. For instance, smoking is recognized as conferring increasing risk of AMD, and the susceptibility is presumed to be due, at least in part, to oxidative processes (43, 44). Consideration also has been given to light-mediated oxidation as a risk factor, and some, but not all, epidemiological studies have been able to establish a relationship (45–47). Some clinical studies (48–50) also have reported that dietary intake or supplemental use of antioxidant vitamins and nutrients can have a beneficial effect on the incidence of AMD. It is thus of potential interest that a number of naturally occurring antioxidants, including vitamins E and C, anthocyanins, and sulfuraphane, have been shown to offer protection against A2E photooxidation (35, 51, 52).

In our microplate assay with solid-form compound, serum incubated with precoated peroxy-A2E and furano-A2E, but not A2E, exhibited elevated levels of iC3b. Nevertheless, from these experiments, it is not possible for us to infer that it is oxygen-containing moieties on oxo-A2E that interact directly with complement. Other than via the oxygen-containing substituents, complement also could be activated by the hydroxyl moiety extending from the pyridinium ring of the molecules. Differences in the orientations of the molecules relative to the hydrophilic polystyrene surface would be expected to determine the portion of the molecule that was exposed to serum. A2E likely would have been oriented with its hydrophilic hydroxyl ($-\text{OH}$) group, forming hydrogen bonds with the hydrophilic polystyrene surface, but a less ordered arrangement could have resulted from oxidation on the side arms of A2E (peroxy-A2E and furano-A2E). In terms of the chemical groups on the oxo-A2E species, it is also important to note that the photooxidation of A2E produces a complex mixture of products that we are only beginning to understand. As we have previously noted, the O–O bond of the endoperoxide moieties can be expected to readily undergo cleavage, yielding a number of intermediates and products including aldehydes (37). One might envision that fragments of A2E produced by photooxidation and containing the pyridinium nitrogen and hydroxyl group of A2E could serve as small nucleophiles capable of hydrolyzing the thioester bond within C3. Further work will be necessary to determine whether activation is by means of the alternative versus classical pathways and to test other bisretinoid lipofuscin pigments (atRAL d-PE and atRAL dimerethanolamine) that we know undergo photooxidation (32).

It is notable that because RPE lipofuscin is sequestered within the lysosomal compartment of the cell, the chemical moieties discussed above are not within immediate reach of complement. However, upon irradiation, A2E becomes photooxidized, and mass spectral analysis indicates that as oxidation proceeds, A2E fragments (Fig. 2). The observation in the present experiments, that complement was activated in serum overlying irradiated-A2E-laden RPE, also is consistent with the view that cleavage products of photooxo-A2E can leave the cell or, in the very least, interact with complement at the cell surface. The amount of A2E that undergoes photooxidation and cleavage in a lifetime may be significant: We have shown that the amount of A2-PE, the immediate precursor or A2E, is severalfold greater than the amounts of A2E that accumulate in RPE cells (53). One explanation for this finding is that normally, a portion of the A2E that forms is lost. Because it is known that levels of A2E in RPE do not diminish under dark conditions (54), it is likely that the light-dependent conditions involve photooxidative processes. Decreased fundus autofluorescence is observed in areas of photoreceptor cell degeneration (55); perhaps this observation can be explained by arrested deposition (due to the absence of photoreceptor cells) coupled with depletion due to photooxidation.

AMD is a disease of the elderly, but it develops progressively over many years before diagnosis. We suggest that photooxidation events initiated in RPE lipofuscin and continuing over time contribute to the inflammatory processes underlying the disease processes. Whether specific constituents of drusen such as amyloid- β (56) and oxidatively modified protein (4) also play a role through complement activation is not known. Also of interest is the possibility of interplay amongst genes that confer susceptibility to inflammation on the one hand and dietary, environmental, and genetic factors that might influence the processes of lipofuscin formation and photooxidation on the other. Our findings lend support to several strategies proposed for the prevention and treatment of AMD, including antioxidant intake (48–50), immunosuppressant therapy (6), and small molecule inhibitors that restrain lipofuscin formation (57, 58).

Materials and Methods

Synthesis of A2E, Peroxy-A2E, and Furano-A2E. A2E was synthesized from atRAL and ethanolamine (2:1) as described (29). To synthesize furano-A2E, A2E (20 mg in 1 ml of methanol) was incubated with MCPBA (11.6 mg; Sigma–Aldrich, St. Louis, MO) and furano-A2E was purified by HPLC as reported in ref. 37. Peroxy-A2E was generated by incubating A2E (15 mg) with 1,4-dimethylnaphthalene endoperoxide (48 mg) (59) in CD₃OD (1 ml), and the oxidation product was purified by reverse-phase HPLC by using a C18 column (10 × 250 mm, 5 mm) and the gradient mode of H₂O and acetonitrile with 0.1% trifluoroacetic acid, as described in ref. 37.

Preparation of Human Serum. Fresh human serum was obtained from blood samples obtained in the absence of anticoagulant. Clotted blood (30 min, room temperature) was centrifuged at 1,500 × g for 10 min, and the collected serum was aliquoted and stored at –80°C.

Cell Culture. Human adult RPE (ARPE-19; American Type Culture Collection, Manassas, VA) cells lacking endogenous A2E (60) were grown in eight-well slide chambers to confluence as reported in refs. 34 and 60. Subsequently, synthesized A2E was introduced to the cultures (10 μ M concentration in medium) for accumulation in the lysosomal compartment of the cells, as formerly described in ref. 60.

Quantitative HPLC and FAB-MS. For the quantification of A2E in cultured cells, the pelleted cells were solubilized in 0.1% Triton

X-100 and extracted three times with chloroform/methanol (2:1). The extract was dried under argon, redissolved in methanol, and analyzed by reverse-phase HPLC (Waters; 2695 HPLC, Model 2996 photodiode array detector) by using a dC18 column (4 × 150 mm) and an acetonitrile and water gradient with 0.1% trifluoroacetic acid (gradient; 90–100%, 0–10 min; 100% acetonitrile, 10–20 min; flow rate, 0.8 ml/min; monitoring at 430 nm). Integrated peak areas were determined by Empower software, and picomolar concentrations were calculated by using external standards of A2E.

To demonstrate A2E photooxidation by FAB-MS, samples of A2E (200 μ M) in PBS (with 0.1% DMSO) were irradiated at 430 nm (\pm 20 nm, 8 mW/cm²) for 1–20 min. FAB-MS was performed on a JOEL JMS-HX110A/110A tandem MS (Akishima, Tokyo, Japan) by using 10-kV acceleration voltage and fitted with an X3 beam FAB gun (6 kV) on the MS-1 ion source and 3-nitrobenzyl alcohol as matrix.

In Vitro Complement Activation. After aspirating the culture medium, A2E-laden RPE were washed with DPBS (GIBCO, Grand Island, NY), and 50 μ l of undiluted human serum was added to each well. The appropriate wells then were irradiated simultaneously at 430 nm (2.6 mW/cm², 30 min) from below, after which they were incubated at 37°C for 30, 60, or 120 min with agitation. For kinetic studies, aliquots of serum were taken at timed intervals. Undiluted nonirradiated serum incubated at 37°C in otherwise empty wells and serum maintained on ice were evaluated for background complement activation. A suspension of Zymosan A (0.25 mg/50 μ l serum; Sigma–Aldrich) served as positive control. Endotoxin (LPS) levels in human serum after incubation with irradiated A2E-containing ARPE-19 cells were determined by chromogenic *Limulus* amoebocyte lysate assay (Associates of Cape Cod, East Falmouth, MA; pyrochrome with diazo reagent for a 540-nm reading; detection limit <0.005 endotoxin units per ml) to be <0.7 endotoxin units per ml.

To coat the wells of 96-well plates with solid-form compound, solutions of A2E, peroxy-A2E, and furano-A2E in methanol (10 and 50 μ g/50 μ l) and methanol alone, were added to the wells, after which the plates were incubated in the dark (37°C, 90 min) to allow solvent evaporation. Once dried, undiluted human serum (50 μ l) was placed in each well, and incubation was continued for 2 h. The concentrations of coated compound were calculated to be 31 and 156 μ g/cm².

Measurement of Complement Activation Products. To measure complement activation, the content of iC3b and C3a were measured in the serum samples by enzyme immunoassay (Quidel Corporation, San Diego, CA). Accordingly, from each serum sample that had been incubated as described above, a 5- μ l aliquot was removed and diluted 1:50 in diluent containing EDTA. The assay used microassay wells precoated with monoclonal antibody to C3a or iC3b, HRP-conjugated anti-human C3a, or iC3b and a chromogenic enzyme substrate with reactivity that could be monitored spectrophotometrically at 405 nm. The optical density obtained for samples of incubated serum (37°C, 2 h) was subtracted from values obtained for other samples and C3a and iC3b standards of known concentrations (micrograms per milliliter) were used for calibration. All samples were assayed in duplicate, and the operator was blinded as to the identity of the samples.

Statistical Analysis. Data were analyzed by one-way ANOVA and Bonferroni's multiple comparison test (Prism; GraphPad, San Diego, CA).

This work was supported by National Institutes of Health Grant EY12951 (to J.R.S.) and a grant from the Steinbach Fund.

1. Hageman GS, Luthert PJ, Chong NHV, Johnson LV, Anderson DH, Mullins RF (2001) *Prog Retin Eye Res* 20:705–732.
2. Davis MD, Gangnon RE, Lee LY, Hubbard LD, Klein BE, Klein R, Ferris FL, Bressler SB, Milton RC, Age-Related Eye Study Group (2005) *Arch Ophthalmol* 123:1484–1498.
3. Curcio CA, Millican CL, Bailey T, Kruth HS (2001) *Invest Ophthalmol Vis Sci* 42:265–274.
4. Crabb JW, Miyagi M, Gu X, Shadrach K, West KA, Sakaguchi H, Kamei M, Hasan A, Yan L, Raybourn ME, et al. (2002) *Proc Natl Acad Sci USA* 99:14682–14687.
5. Nozaki M, Raisler BJ, Sakurai E, Sarma JV, Barnum SR, Lambris JD, Chen Y, Zhang K, Ambati BK, Baffi JZ, Ambati J (2006) *Proc Natl Acad Sci USA* 103:2328–2333.
6. Donoso LA, Kim D, Frost A, Callahan A, Hageman G (2006) *Surv Ophthalmol* 51:137–152.
7. Zarepari S, Buraczynska M, Branham KE, Shah S, Eng D, Li M, Pawar H, Yashar BM, Moroi SE, Lichter PR, et al. (2005) *Hum Mol Genet* 14:1449–1455.
8. Seddon JM, Gensler G, Milton RC, Klein ML, Rifai N (2004) *J Am Med Assoc* 291:704–710.
9. Black S, Kushner I, Samols D (2004) *J Biol Chem* 279:48487–48490.
10. Haines JL, Hauser MA, Schmidt S, Scott WK, Olson LM, Gallins P, Spencer KL, Kwan SY, Nouredine M, Gilbert JR, et al. (2005) *Science* 308:419–421.
11. Edwards AO, Ritter R, Abel KJ, Manning A, Panhuysen C, Farrer LA (2005) *Science* 308:421–424.
12. Klein RJ, Zeiss C, Chew EY, Tsai JY, Sackler RS, Haynes C, Henning AK, SanGiovanni JP, Mane SM, Mayne ST, et al. (2005) *Science* 308:385–389.
13. Hageman GS, Anderson DH, Johnson LV, Hancox LS, Taiber AJ, Hardisty LI, Hageman JL, Stockman HA, Borchoradt JD, Gehrs KM, et al. (2005) *Proc Natl Acad Sci USA* 102:7227–7232.
14. Gold B, Merriam JE, Zernant J, Hancox LS, Taiber AJ, Gehrs K, Cramer K, Neel J, Bergeron J, Barile GR, et al. (2006) *Nat Genet* 38:458–462.
15. Seddon JM, George S, Rosner B, Rifai N (2005) *Arch Ophthalmol* 123:774–782.
16. Law SKA, Reid KBM (1995) *Complement* (Oxford Univ Press, Oxford).
17. Morgan BP, Harris CL (1999) *Complement Regulatory Proteins* (Academic, San Diego).
18. Rother K, Till GO (1988) *The Complement System* (Springer, Berlin).
19. Bhakdi S, Torzewski M, Paprotka K, Schmitt S, Barsoom H, Suriyaphol P, Han S-R, Lackner KJ, Husmann M (2004) *Circulation* 109:1870–1876.
20. Sim RB, Day AJ, Moffatt BE, Fontaine M (1993) *Methods Enzymol* 223:13–35.
21. Wieland E, Dorweiler B, Bonitz U, Lieser S, Walev I, Bhakdi S (1999) *Eur J Clin Invest* 29:835–841.
22. Demacker PNM (1999) *Eur J Clin Invest* 29:811–813.
23. Daly J, Kotwal GJ (1998) *Neurobiol Aging* 19:619–627.
24. Noordin S, Shortkroff S, Sledge CB, Spector M (2004) *Biomaterials* 25:5347–5352.
25. DeHeer DH, Engels JA, De Vries AS, Knapp RH, Beebe JD (2001) *J Biomed Mater Res* 54:12–19.
26. Salvador-Morales C, Flahaut E, Sim E, Sloan J, Green MLH, Sim RB (2006) *Mol Immunol* 43:193–201.
27. Delori FC, Goger DG, Dorey CK (2001) *Invest Ophthalmol Vis Sci* 42:1855–1866.
28. Sakai N, Decatur J, Nakanishi K, Eldred GE (1996) *J Am Chem Soc* 118:1559–1560.
29. Parish CA, Hashimoto M, Nakanishi K, Dillon J, Sparrow JR (1998) *Proc Natl Acad Sci USA* 95:14609–14613.
30. Liu J, Itagaki Y, Ben-Shabat S, Nakanishi K, Sparrow JR (2000) *J Biol Chem* 275:29354–29360.
31. Ben-Shabat S, Parish CA, Vollmer HR, Itagaki Y, Fishkin N, Nakanishi K, Sparrow JR (2002) *J Biol Chem* 277:7183–7190.
32. Fishkin N, Sparrow JR, Allikmets R, Nakanishi K (2005) *Proc Natl Acad Sci USA* 102:7091–7096.
33. Sparrow JR, Boulton M (2005) *Exp Eye Res* 80:595–606.
34. Sparrow JR, Zhou J, Ben-Shabat S, Vollmer H, Itagaki Y, Nakanishi K (2002) *Invest Ophthalmol Vis Sci* 43:1222–1227.
35. Sparrow JR, Vollmer-Snarr HR, Zhou J, Jang YP, Jockusch S, Itagaki Y, Nakanishi K (2003) *J Biol Chem* 278:18207–18213.
36. Ben-Shabat S, Itagaki Y, Jockusch S, Sparrow JR, Turro NJ, Nakanishi K (2002) *Angew Chem Int Ed* 41:814–817.
37. Jang YP, Matsuda H, Itagaki Y, Nakanishi K, Sparrow JR (2006) *J Biol Chem* 280:39732–39739.
38. Dillon J, Wang Z, Avalle LB, Gaillard ER (2004) *Exp Eye Res* 79:537–542.
39. Takada N, Watanabe M, Yamada A, Suenaga K, Yamada K, Ueda K, Uemura D (2001) *J Nat Prod* 64:356–359.
40. Mags JL, Bishop LPD, Batty KT, Dodd CC, Ilett KF, O'Neill PM, Edwards G, Park BK (2004) *Chem Biol Interact* 147:173–184.
41. Allikmets R, Singh N, Sun H, Shroyer NF, Hutchinson A, Chidambaram A, Gerrard B, Baird L, Stauffer D, Peiffer A, et al. (1997) *Nat Genet* 15:236–246.
42. Zhou J, Cai B, Jang YP, Pachydaki S, Schmidt AM, Sparrow JR (2005) *Exp Eye Res* 80:567–580.
43. Smith W, Mitchell P, Leeder SR (1996) *Arch Ophthalmol* 114:1518–1523.
44. Age-Related Eye Disease Study Research Group (2000) *Ophthalmol* 107:2224–2232.
45. Cruickshanks KJ, Klein R, Klein BEK, Nondahl DM (2001) *Arch Ophthalmol* 119:246–250.
46. Taylor HR, West S, Munoz B, Rosenthal FS, Bressler SB, Bressler NM (1992) *Arch Ophthalmol* 110:99–104.
47. Tomany SC, Cruickshanks KJ, Klein R, Klein BEK, Knudtson MD (2004) *Arch Ophthalmol* 122:750–757.
48. Christen WG, Ajani UAA, Glynn RJ, Manson JE, Schaumberg DA, Chew EC, Buring JE, Hennekens CH (1999) *Am J Epidemiol* 149:476–484.
49. Age-Related Eye Disease Study Research Group (2001) *Arch Ophthalmol* 119:1417–1436.
50. van Leeuwen R, Boekhoorn S, Vingerling JR, Witteman JC, Klaver CC, Hofman A, de Jong PT (2005) *J Am Med Assoc* 294:3101–3107.
51. Zhou J, Gao X, Cai B, Sparrow JR (2006) *Rejuvenation Res* 9:256–263.
52. Jang YP, Zhou J, Nakanishi K, Sparrow JR (2005) *Photochem Photobiol* 81:529–536.
53. Kim SR, Nakanishi K, Itagaki Y, Sparrow JR (2006) *Exp Eye Res* 82:828–839.
54. Mata NL, Weng J, Travis GH (2000) *Proc Natl Acad Sci USA* 97:7154–7159.
55. Von Ruckmann A, Fitzke FW, Fan J, Halfyard A, Bird AC (2002) *Am J Ophthalmol* 133:780–786.
56. Dentchev T, Milam AH, Lee VMY, Trojanowski JQ, Dunaief JL (2003) *Mol Vis* 9:184–190.
57. Maiti P, Kong J, Kim SR, Sparrow JR, Allikmets R, Rando RR (2006) *Biochemistry* 45:852–860.
58. Radu RA, Han Y, Bui TV, Nusinowitz S, Bok D, Lichter J, Widder K, Travis GH, Mata NL (2005) *Invest Ophthalmol Vis Sci* 46:4393–4401.
59. Turro NJ, Chow M-F, Rigaudy J (1981) *J Am Chem Soc* 103:7218–7222.
60. Sparrow JR, Parish CA, Hashimoto M, Nakanishi K (1999) *Invest Ophthalmol Vis Sci* 40:2988–2995.